

Device for Generation of Megaampere Current Pulses with a 10^{-7} s Rise Time in Radiating Load of the GIT 12 Generator

V.A. Kokshenev, F.I. Fursov, and N.E. Kurmaev

Institute of High Current Electronics, SB, RAS, Tomsk, Russia
E-mail: vak@oit.hcei.tsc.ru

Abstract – A device for switching a current of amplitude 4–5 MA to a load upstream of a plasma opening switch has been developed and tested. The device consists of a microsecond plasma opening switch (MPOS), a multichannel post-hole convolute and a controllable closing switch with a surface discharge. The MPOS has been designed in the form of a double coaxial with an intermediate electrode – cathode transparent to plasma. This makes it possible to increase the charge switched in the MPOS, to minimize the inductance of the MPOS-load region, and thus to enhance the amplitude of the switching current.

1. Introduction

An inductive energy store in combination with an opening switch is a simple and cheap method of power amplification in a load. Plasma opening switches of the PFS type (plasma flow switches) or microsecond plasma opening switches (MPOS's) are best suited to radiating Z-pinch loads. Each of them has its own advantages and shortcomings. So, experiments with MPOS's have revealed a decrease in MPOS resistance in the open state with increasing switched charge during the conduction phase [1, 2]:

$$R_{so} \times Qc \cong \text{const},$$

where $Qc \sim (Ic \times tc)$ is the current passed through the MPOS by the moment the switch resistance begins to increase (Ic is the MPOS current amplitude, tc is the conduction phase duration), R_{so} is the MPOS resistance averaged over the time of energy delivery into a load. This fact calls into question the use of MPOS's in the multimegaampere range and stimulates the search for new possible ways of settling the problem.

At $Ic \sim 107$ A, $tc \sim 1$ μ s, the experimental dependence for R_{so} gives $\sim (0.3-0.5)$ Ω . For a current rise time of $\sim 10^{-7}$ s at the load, the inductance of the MPOS-load circuit should be $Lsz \leq 20$ nH. To attain high values of $(Ic \times tc)$, it is necessary to increase the MPOS dimensions and to initiate high-velocity plasma flows, which would propagate from the MPOS zone along the power flow. With the traditional arrangement of a load downstream of a plasma opening switch, the load should be moved away from the switch. These facts increase Lsz . The above trouble can be cleared up by connecting the load upstream of

the MPOS. This way of load connection has proven its capabilities in experiments on the MARINA setup with an ion diode [3] and on the GIT-4 generator with inductive loads [4]. In both cases, no considerable change has been found in the MPOS characteristics on switching part of the current with associated decrease in magnetic field at the cathode.

This paper describes the design of the device and presents the results obtained in experiments.

2. Experimental Arrangement

One of the possible ways of connecting a load upstream of a MPOS is the use of a post-hole convolute with symmetric current lead into the load. Schematic of this design is shown in Fig. 1, a. The system consists of a coaxial cross-input, which is a multichannel post – hole cathode-anode convolute 2, and load 4 located through the center. For connecting the load, use is made of closing switch 3 with a vacuum surface discharge.

The design has been optimized with respect to the channel size, electrode gaps, and the number of channels (12, 6). The post-hole convolute consisting of six channels with a post to hole diameter ratio of 36 mm/14 mm has demonstrated the smallest losses ($\leq 10\%$) in the maximum of the magnetic field (see Fig. 1, b). In so doing, the current amplitude in each channel was up to 800 kA. The post-hole convolute was tested at a voltage of up to 1.5 MV.

For the design with a post-hole convolute, a MPOS has been developed which consists of two coaxial opening switches S1 and S2 operating in synchrony. The switches have common transparent cathode 1 and a plasma source. Plasma is produced by two rows of plasma guns (PG's), 32 PG's each, on a \varnothing 500-mm anode and is delivered to electrode gap S2 through electrode gap S1 and rod cathode 1. This allows a more efficient use of the plasma source and a decrease in the inductance of the switch-load region. Anodes 5 of both MPOS parts have an vane design: 32 external vanes and 24 internal vanes. This was done to improve the contact with the switch plasma, to accelerate more effectively this plasma to the free spread region, and to provide a possibility of its "forcing out" from the electrode gap. The rod electrodes decrease the area where the MPOS-produced particle beams arrive that is conceivably responsible for the slower closure of the MPOS gap [1, 7].

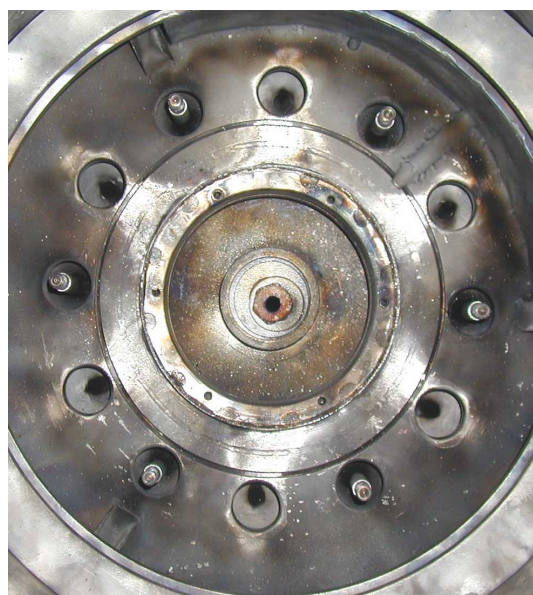
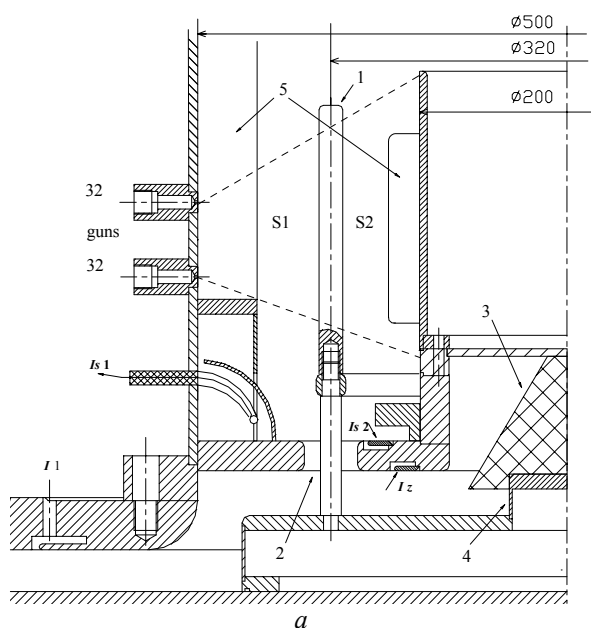


Fig. 1. *a* – design of the device: S1, S2 – electrode gaps of the opening switch, 1 – cathode rods, 2 – channel of the post-hole convolute, 3 – insulator of the closing switch, 4 – load, 5 – anode vanes; *b* – photo of the post-hole convolute anode diaphragm after tests: traces of electron leakages in the form of 6 light rays in the center between 6 posts

The equivalent electric circuit used in the experiment is shown in Fig. 2. The possibility of measuring the currents in all branches of the circuit and the post-hole convolute voltage allowed measuring or calculating all main parameters of the transient process and the parameters of the circuit elements. The choice of differentiating sensors for measuring the current was made to register more accurately the processes in the loops with nonlinear elements. The procedure of experimental and calculation data processing was similar to the one described elsewhere [1, 4].

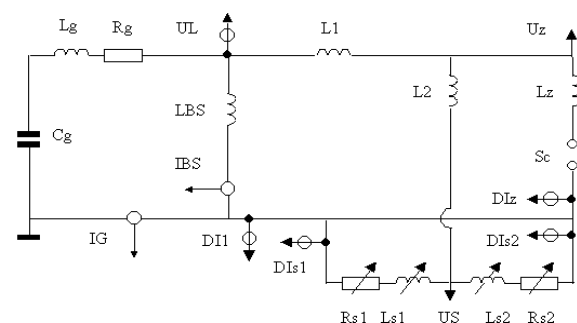


Fig. 2. Electric circuit in GIT-12 experiment: $C_g = 14.4 \mu\text{F}$, $L_g \cong 89 \text{ nH}$, $R_g \cong 0.04 \Omega$ – capacitance, inductance, and resistance of the energy store; $L_1 = 10 \text{ nH}$ – invariant part of the inductance above the $\varnothing 1.5 \text{ m}$ electrode assembly; $LBS = 424 \text{ nH}$ – inductive voltage divider; $L_2 \cong 8.3 \text{ nH}$ – inductance of the post-hole convolute circuit up to the PG plane; $L_{s1}, R_{s1}, L_{s2}, R_{s2}$ – inductance and resistance of the opening switches; $L_z \cong 15 \text{ nH}$ – inductance of the load circuit; IG, IBS – Rogowskii coil; UL – voltage across the GIT12 collector; $DI1, DI1s, DIz$ – current derivative sensors

3. Results

At the first stage the proposed MPOS(S1 + S2) version was tested, and its characteristics were compared with a traditional coaxial MPOS(S0). To this end, we used an opaque screen on the cathode. The experiments were performed in no-load conditions at a high output voltage (480 kV) of the Marx generator. In this experiment, the load for the inductive energy store was the MPOS itself. The current amplitude and the duration of the MPOS conduction phase were controlled by varying the time delay t_d between the operation of the plasma guns and triggering of the Marx generator.

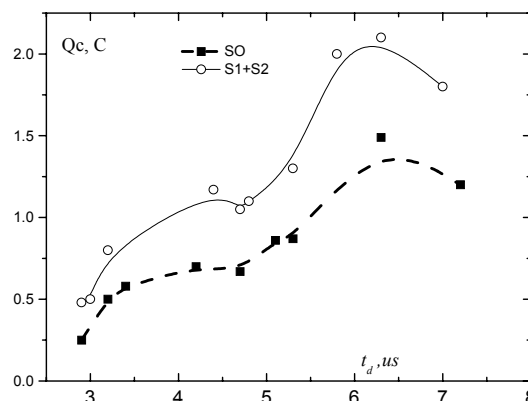


Fig. 3. Characteristics of the MPOS during the conduction phase: S0 – switch with a nontransparent cathode, (S1 + S2) – switch with a transparent cathode

The use of the common plasma flow from 64 PG's in both electrode gaps S1 and S2 makes it possible to increase the charge switched in the MPOS by a factor of ~ 1.5 : $Q_c(S1 + S2) \cong 1.5 Q_c(S0)$. Fig. 3 shows the MPOS charge within the conduction phase versus the time delay t_d for the design with a transparent cathode

(S1 + S2) and for the version (S0) where the cathode is solid and there is no plasma in the gap S2. Fig. 4 presents the characteristics of two versions of the opening switch in the high-voltage phase.

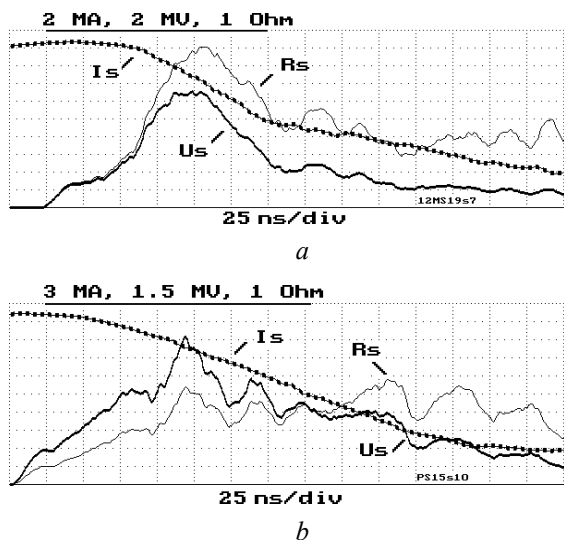


Fig. 4. Characteristic curves of the MPOS current, voltage and its resistance: S0 – a; (S1+S2) – b

The increase in the plasma amount in the gap S2 is due to the increase in cathode transparency. In this connection, we studied the effect of the cathode design on the MPOS characteristics. Fig. 5 shows the dependence of the MPOS conduction current amplitude on the time delay t_d for three versions of the cathode: 1–12 \varnothing 16-mm rods with a geometric transparency $\alpha = 81\%$, 2–24 \varnothing 16-mm rods with $\alpha = 62\%$, and 3–12 \varnothing 16-mm rods covered with a grid of total transparency $\alpha = 52\%$. It can be seen that for the variant with a rod cathode of maximum transparency the conduction current amplitude is saturated. In this case, besides the decreasing cathode area, there are maximum linear current densities (up to 50 kA/cm) over the cathode rods. The high values of the magnetic field at the cathode should reduce the duration of the conduction phase, all other factors being equal, as it takes place when decreasing the cathode diameter in the coaxial MPOS [5, 6]. A similar process was observed with a decreased number of cathode rods that indirectly supported the prevailing effect of the near-cathode processes on the conduction phase.

Experiments with current switching to a low-impedance load. The circuit of connecting a load upstream of a MPOS requires a closing switch. First, this switch serves to insulate the load from the voltage U_z equal to the sum of voltages across the inductor L_2 and MPOS during the conduction phase: $U_z = U_{L_2} + U_s$. And second, it should provide effective current switching to a load at the optimal moment in time. This imposes calls for the minimum possible inductance and resistance in switching, controllability, and a reasonable lifetime at a current amplitude of up to 4÷5 MA.

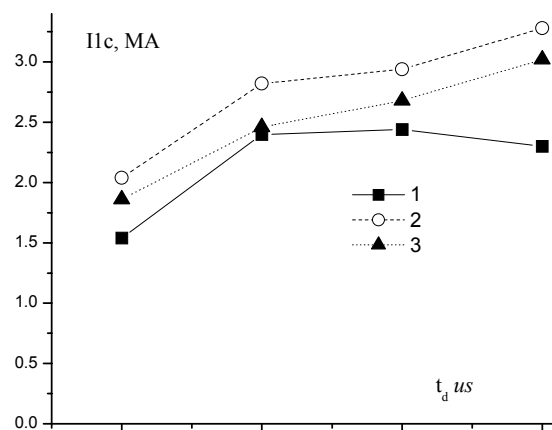


Fig. 5. Effect of the cathode design on the MPOS(S1 + S2) characteristics during the conduction phase: 1 – 12 rods \times \varnothing 16 mm, $\alpha = 81\%$; 2 – 24 rods \times \varnothing 16 mm, $\alpha = 62\%$; 3 – 12 rods \times \varnothing 16 mm + grid, $\alpha = 52\%$

Several versions of the controllable closing switch and of that operating in the self-breakdown mode have been tested. No satisfactory results have been obtained for vacuum closing switches either with plasma flow arrived from the MPOS regions or produced by additional plasma guns. Current prepulses were normally observed at the load or the time the switch was in the low-resistance state was greatly shorter than the current risetime at the load or both. The switch with a surface discharge ensure much netter characteristics. Fig. 6 shows waveforms for the switch design presented in Fig. 3.

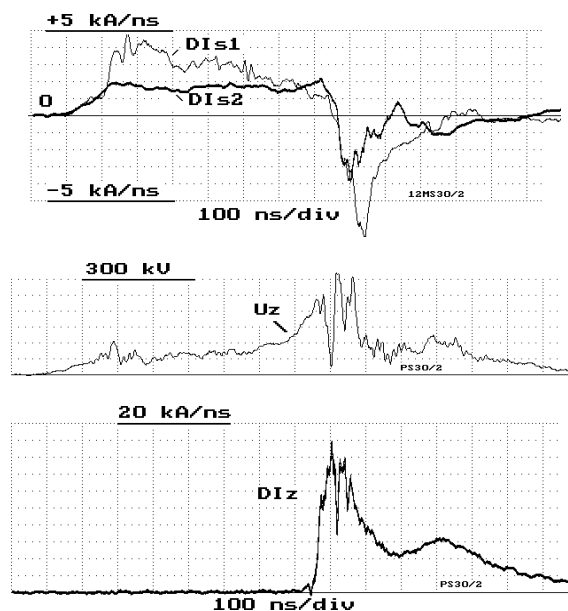


Fig. 6. Waveforms of the current derivative in both parts of the switch $DI s_1$, $DI s_2$, in the load $DI z$ and the voltage U_z across the load with a closing switch

Experiments on current switching to a low-impedance load have shown that there exists an optimal moment at which the closing switch operates.

That is before part of the current has left the opening switch some energy should be liberated in it, including the energy expended for plasma erosion, to attain the initial resistance required for efficient current switching to the load. With the design shown in Fig. 3, which ensures an acceptable level of the load circuit inductance (~ 15 nH), we have not managed to control in full measure the moment at which the closing switch is broken down due to the electric strength of the insulator surface.

The maximum rates of increase in load current were obtained for a controllable closing switch. The design of this switch is presented in Fig. 7, *a*. The switch chamber consists of two parts. Rod surface plasma sources (flashboards, FB's) 1 are uniformly located in volume I along the azimuth. The vane separation of the rods is such that the flashboard- insulator separation is 15 mm. On the operation of FB's with simultaneous production of powerful UV by 24 spark gaps, a plasma flow with a front moving from the anode to the insulator surface with a velocity of ~ 107 cm/s is initiated. When the anode potential is "carried out" to the insulator surface the insulator is overlapped in the region of diaphragm 2 between volumes I and II. The closing switch allowed current switching to the low-impedance load of volume II at the optimal moment in time when there was a maximum rate of increase in opening switch voltage. As can be seen from the oscillogram of U_z in Fig. 7, *b*, the closing switch was broken down at a voltage of ~ 320 kV.

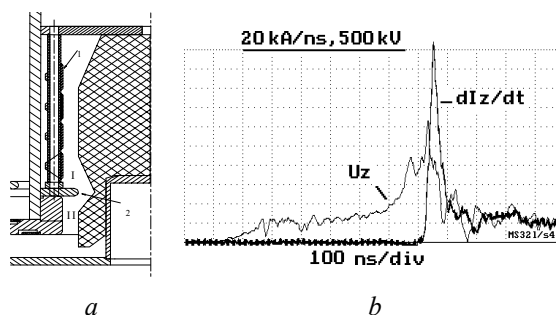


Fig. 7. *a* – design of the controllable closing switch, *b* – oscillograms of the voltage across the switch and load U_z and the load current derivative dz/dt

Experiments with the controllable switch confirm the influence of the moment of switching on the MPOS resistance. Fig. 8 shows the MPOS(S0) characteristics for two versions of load connection ($L_z \cong 20$ nH). Curve 1 corresponds to the mode where the voltage U_z is appreciably higher than its value during the conduction phase and the rate of its increase is high, too. Plot 2 corresponds to the mode where the switch operates at the initial stage of increase in U_z at small dU_z/dt . Switching the load in mode 2 shortens the high-resistance phase of the

MPOS and is characterized by smaller values of dz/dt .

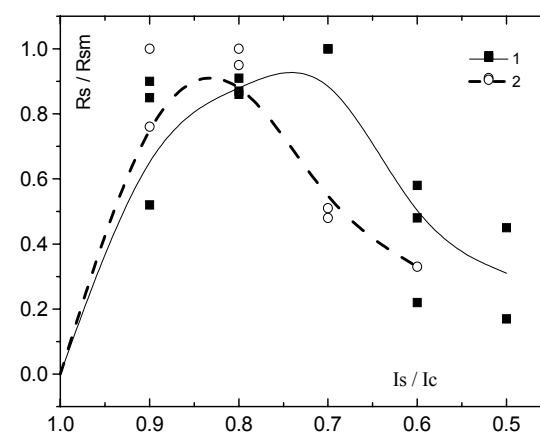


Fig. 8. Current-dependence of the normalized MPOS(S0) resistance (I_c and R_{sm} – amplitude of the MPOS current and resistances): 1 – $dU_z/dt \sim \max$; 2 – switching in mode 2

4. Conclusion

An MPOS design with a cathode transparent to plasma has been proposed. The design allows increasing the charge switched during the conduction phase by a factor of 1.5 and makes it possible to optimize the inductance of the MPOS-load region. As a result, the amplitude of the current whose symmetric cross-input is provided by the six-channel post-hole convolute has been increased. The use of a controllable closing switch in a load circuit of inductance ~ 15 nH has allowed a current increasing with > 20 kA/ns. The results obtained and the possibility of increasing the output voltage of the Marx generator to 720 kV provide a basis for production of current with an amplitude of ≥ 4 MA and a risetime $\sim 10^{-7}$ s at radiating loads.

References

- [1] V.A. Kokshenev, N.E. Kurmaev, F.I. Fursov, in: *Proc. 12th Symp. High Current Electronics*, 2000, pp. 268–273.
- [2] P.S. Ananjin, B.M. Kovalchuk, V.A. Kokshenev et al., in: *Proc. X Intern. Conf. on High Power Particle Beams*, 1994, pp. 311–314.
- [3] E.N. Abdullin, et al., *Rus. J. Plasma Physics* **13**(9), 1027 (1987).
- [4] A.N. Batrikov, A.A. Zheritsin, A.A. Kim et al., *Rus. Izv. Wuzov. Physika* **42**(12), 31 (1999).
- [5] V.A. Kokshenev, in: *Pros. VIIth Symposium on High Current Electronics*, Tomsk Russia, 1988, pp. 142–144.
- [6] A.S. Chuvatin, A.A. Kim, V.A. Kokshenev et al., *Rus. Izv. Wuzov. Physika* **40**(12), 56 (1997).
- [7] B.M. Kovalchuk, V.A. Kokshenev, A.A. Kim et al., *J. Tech. Physics (Warszawa)* **39**, 121 (1998).